COMMUNICATION

A novel aptameric nanobiosensor based on self-assembled DNA-MoS₂ nanosheet architecture for biomolecule detection

## Jia Ge, En-Cai Ou, Ru-Qin Yu*, and Xia Chu*

We have developed a novel fluorescence-activated DNA-MoS₂ nanosheet biosensor for detecting biomolecular targets such as proteins and small molecules based on a self-assembled architecture of DNA aptamer and MoS₂ nanosheet. The 10 proposed design is simple to prepare and exhibits low background interference, high sensitivity and rapid response.

Aptamers are short, single-stranded oligonucleotides generated from an *in vitro* method known as SELEX (systematic evolution of ligands by exponential enrichment).[1-3] They possess 15 high specificity in molecular recognition to targets ranging from small organic or inorganic substances to even proteins or cells.[4-9] Compared with antibodies, the prominent advantage of aptamer-based method is that oligonucleotides can be synthesized chemically with ease and accuracy at low cost. They are 20 controllable in modification to fulfill different diagnostic and therapeutic purposes, possessing a series of excellent properties such as nice stability during long-term storage, the ability to sustain reversible denaturation, low toxicity, lack of immunogenicity, and fast tissue penetration.[10] Aptamers have 25 been extensively utilized to construct various biosensors for different biomolecular targets.[11-16] Fluorescent aptasensors are particularly useful and popular, in part due to their high sensitivity and feasibility of quantification.[17, 18]

MoS₂ nanosheets, an emerging two-dimensional (2-D)-30 layered material analogous to graphene,[19] have been attracting much attention because of its excellent nanoelectronics, optoelectronics, and energy harvesting properties.[20-24] Compared with graphene, MoS₂ nanosheets can be synthesized in a large scale, and can be directly dispersed in aqueous solution without 35 the aid of surfactants, implying that MoS₂ nanosheets will hold great promise as a novel nanomaterial for biomedical applications. Nevertheless, the use of MoS₂ nanosheets as a bioanalytical platforms has been largely unexplored. Very recently, MoS₂ nanosheets were demonstrated to be able to spontaneously adsorb 40 single-stranded DNA by the van der Waals force between nucleobases and the basal plane of MoS₂ nanosheets, acting as an efficient dye quencher for a two-step assay of DNA and small molecules.[25]

Herein, we reported for the first time that an aptamer probe 45 can be self-assembled on the surface of a MoS₂ nanosheet to form a stable aptamer–MoS₂ nanosheet architecture, and the nano-assembly retains the binding affinity and specificity of the

aptamer to its target. Moreover, binding of the aptamer probes to the target can release the aptamer away from the MoS₂ nanosheet. 50 Hence, the nanoassembly allows the development of novel DNA-MoS₂ nanosheet biosensor for single-step detection of different targets, as shown in Scheme. 1. After the aptamer probe with a fluorophore label at its terminal is assembled on the MoS₂ nanosheet, the fluorescence of the fluorophore label is largely 55 quenched due to possible electron or energy transfer between the closely contacted dye molecules and the MoS₂ nanosheet.[25] In the presence of the target, the specific binding between the dye-labeled aptamer with its target induces the formation of a more rigid conformation such as DNA duplex or quadruplex. Such a 60 rigid conformation will mitigate van del Waals force between the aptamer and the MoS₂ nanosheet, releasing the aptamer probes from the nanosheet surface and activating the fluorescence signal. To demonstrate the developed strategy, we choose adenosine triphosphate (ATP) and human α-thrombin as the model. The 65 result revealed that the aptamer–MoS₂ nanoassembly provides an ideal and versatile biosensor for sensing different analytes.
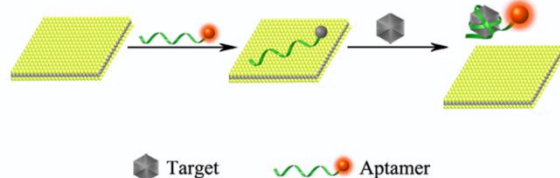
Scheme. 1. Schematic illustration of using MoS₂ nanosheet as an effective sensing biosensor.

70

MoS₂ nanosheets prepared by chemical exfoliation according to Eda method[26] were characterized by transmission electron microscopy (TEM), atomic force microscopy (AFM), and X-ray diffraction (XRD). Stable dispersions of MoS₂ 75 nanosheets were obtained in aqueous solutions, no sediment observed even after the MoS₂ nanosheets were stored for more than one week (Fig. 1). A negative ζ potential of -27.1 mV was observed for the nanosheets (Fig. S1 in ESI), indicating a negative charge on the MoS₂ nanosheet surfaces. XRD patterns 80 revealed that there was no (002) reflection for the nanosheets (Fig. 2A). AFM characterization of the as-prepared MoS₂ nanosheets

indicated that the thickness of the nanosheets was ~1.6 nm, evidencing the successful synthesis of the two-layer MoS_2 nanosheets.
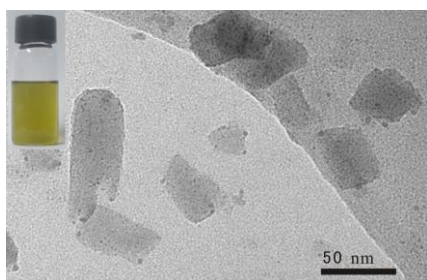

Fig. 1. Typical TEM image of prepared MoS_2 nanosheets and photograph of a typical chemically exfoliated MoS_2 suspension in water.
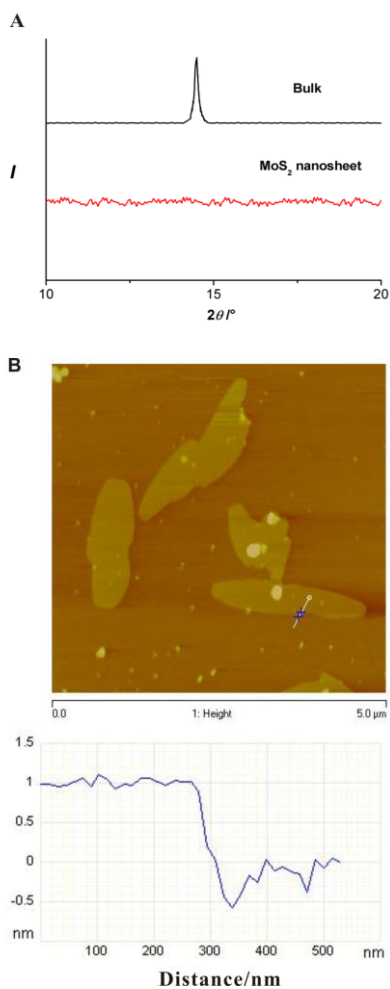

Fig. 2. (A) Comparison of XRD patterns of bulk MoS_2 and MoS_2 nanosheets. (B) Typical AFM image and associated height profile of MoS_2 nanosheets.

Fig. 3A shows typical emission spectra response of FAM-labeled ATP aptamer P1. In the absence of MoS_2 nanosheets, the fluorescence spectrum of P1 exhibits strong fluorescence emission (curve a). However, the addition of MoS_2 nanosheets leads to the quenching of fluorescence up to 94% (curve e), revealing that MoS_2 nanosheets can strongly adsorb FAM-labeled P1 and quench the fluorescence very effectively. Upon the addition of ATP, the solution showed significant fluorescence restoration (curve b). Compared with P1, FAM-labeled control DNA sequence P3 was also adsorbed on the MoS_2 nanosheets, resulting in a quenched fluorescence signal (curve d). With the addition of ATP, the solution still displayed a very weak fluorescent signal (curve c). Therefore, we concluded that the fluorescence restoration was caused only by specific interaction between ATP and its aptamer, although the fluorescence cannot be recovered by 100% for the fact that part of the aptamer, when assembled on MoS_2 nanosheets, may fold into incorrect conformations and cannot bind to its target. The kinetic behaviour of the designed DNA-MoS_2 nanosheet biosensor was investigated by monitoring the fluorescence intensity as a function of time. The data revealed a rapid response of the biosensor to ATP in which the fluorescence signal reached up to 88% of the saturated response within 10 min (Fig. S2 in ESI).
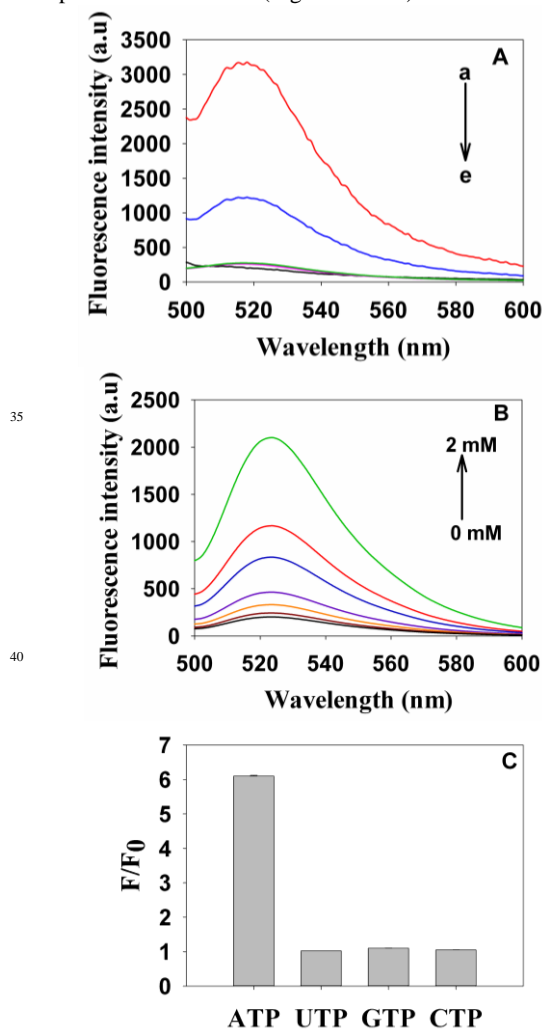
Fig. 3. (A) Fluorescence emission spectra of P1 and P3 under different conditions: (a) P1; (b) P1 + MoS_2 + ATP; (c) P3 + MoS_2 + ATP; (d) P3 + MoS_2; (e) P1 + MoS_2 (MoS_2 40 μg mL^{-1}, P1 50 nM, P3 50 nM, ATP 1 mM). (B) Fluorescence emission spectral responses of DNA-MoS_2 nanosheet biosensor to varying concentrations of ATP, 0, 10, 50, 100, 500, 1000, and 2000 μM, respectively. (C) Peak fluorescence intensity enhancement (F/F_0) of DNA-MoS_2 nanosheet biosensor in the presence of 1000 μM ATP, UTP, GTP or CTP, respectively (MoS_2 40 μg mL^{-1}, P1 50 nM).

It was found that the amount of MoS_2 nanosheets used in the

assay has substantial effect on the fluorescence quenching responses (Fig. S3 in ESI). The fluorescence responses in the presence of MoS_2 nanosheets of different concentrations were examined. The increased amount of MoS_2 nanosheets gave
5 decreased blank signals with a concomitant decrease of the fluorescence responses, and the best signal-to-background ratio was obtained with 40 µg mL^{-1} MoS_2 nanosheets. Such observations could be ascribed to the weak adsorption of DNA duplex or quadruplex on MoS_2 nanosheet surfaces which became
10 dominant in the presence of excessive MoS_2 nanosheets. As a result, 40 µg mL^{-1} was used as the optimized concentration for MoS_2 nanosheets.

It was observed in Fig. 3B that the fluorescence responses of the aptamer–MoS_2 nanosheet assembly dramatic increased with
15 increasing concentrations of ATP in the range from 0 to 2000 µM. The peak fluorescence intensity ratio F/F_0 plotted against the concentration of ATP (Fig. S4 in ESI), where F was the peak fluorescence intensity in the present of target, and F_0 was the peak fluorescence intensity of blank. The linear range covers
20 from 10 to 2000 µM (regression coefficient R^2 = 0.998) with the detection limit estimated to be 4 µM according to the 3σ rule. These results clearly demonstrate that the fluorescence intensity of P1 is sensitive to ATP concentration, i.e. higher concentration of ATP leads to higher fluorescence intensity. This DNA-MoS_2
25 nanosheet biosensor shows excellent detection performance comparable to the previously reported by aptamer/graphene oxide nanosheets sensing platform.[27]

We also examined the selectivity of this DNA-MoS_2 nanosheet biosensor for ATP detection. As shown in Fig 3C, a
30 fluorescence enhancement of F/F_0 = 6.08 was obtained in the present of 1000 µM ATP. In contrast, the fluorescence signals had little significant change in present of 1000 µM CTP, GTP, or UTP. The related fluorescence enhancement of F/F_0 was 1.04, 1.21 or 1.05, respectively. The result indicated that the proposed
35 DNA-MoS_2 nanosheet biosensor had excellent selectivity toward ATP, which was contributed by the nature of high selectivity of aptamer.

To demonstrate the feasibility of the proposed strategy in assays with complex biological matrix, we investigated the
40 performance of the DNA-MoS_2 nanosheet biosensor in detection of ATP in blood serum. Different samples were prepared by add ATP with a certain concentration into 1% human serum. Obviously, the fluorescence responses of the biosensor to different concentrations of ATP in human serum were similar to
45 that observed in Tris-HCl buffer (Fig. S5 in ESI). These results, thus, exhibited that the developed biosensor was still highly selective to ATP under a complex biological matrix.

Additionally, a further experiment was performed to analyze cellular ATP in human lung adenocarcinoma A549 cell
50 extractions. Significant fluorescence enhancement was obtained in freshly prepared cell extraction (Fig. S6, curve a in ESI). In contrast, a slight fluorescence signal comparable with the blank was observed in the cell extraction after 24 h aging (Fig. S6, curve b in ESI). The concentration of ATP in the fresh cell
55 extractions was estimated to be 1.11 ± 0.08 mM (n = 2), and 0.12 ± 0.01 mM (n = 2) for cell extractions after 24 h aging, which were agreed with those obtained using commercial ATP assay kit (Table S1 in ESI). It clearly revealed the DNA-MoS_2 nanosheet

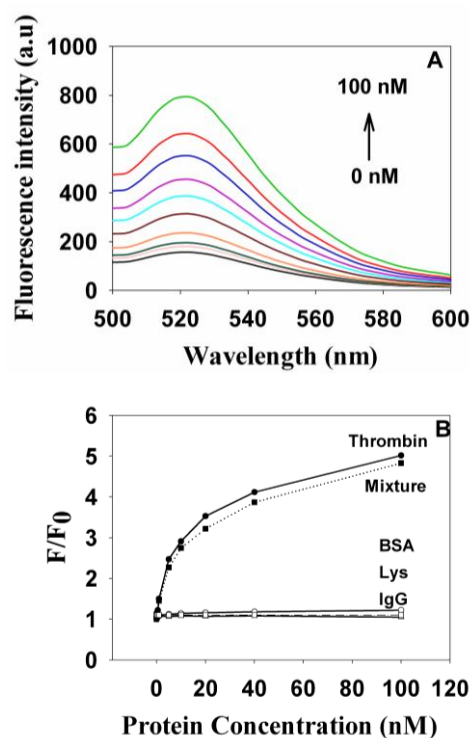biosensor might be a promising strategy ATP assays.

60

Fig. 4. (A) Fluorescence emission spectra of DNA-MoS_2 nanosheet biosensor in the presence of increasing amounts of thrombin. The arrow indicates the signal changes with increases in thrombin concentrations (0, 0.5, 1, 2, 3, 5, 10,
65 20, 40, 100 nM). (B) Fluorescence enhancements (F/F_0) of DNA-MoS_2 nanosheet biosensor in the Tris-HCl buffer by increasing concentrations of thrombin (●), BSA (○), Lys (□), and IgG (△), separately, as well as a mixture of proteins (concentrations of proteins were 100 nM) with increasing concentrations of thrombin (■). Fluorescence intensity ratio F/F_0 plotted
70 against the concentration of protein, where F and F_0 are the fluorescence intensity with and without protein (MoS_2 40 µg mL^{-1}, P2 20 nM).

In order to investigate the generalization of the proposed strategy, based on the same principle DNA-MoS_2 nanosheet
75 biosensor using the aptamer against thrombin was designed for human α-thrombin targeting. As expected, in the absence of thrombin, FAM-labeled aptamer P2 did not emit dye fluorescence; however, in the presence of the thrombin, strong dye emission with a fluorescence intensity enhanced up to 5.01 times upon the
80 addition of 100 nM thrombin was observed (Fig. S7 in ESI). The fluorescence intensity dramatic increased with increasing concentrations of thrombin was also observed, as shown in Fig. 4A. A detection limit of 300 pM was achieved (according to the 3σ rule), which was lower than that obtained using graphene (2
85 nM)[7] or single-walled carbon nanotube (1.8 nM)[28] fluorescent aptasensors. The selectivity of sensor was also investigated by employing nonspecific target proteins. Fig. 4B shows the fluorescence intensity ratio F/F_0 of the DNA-MoS_2 nanosheet biosensor when incubated with Lys, bovine serum albumin
90 (BSA), human IgG or mixture proteins. Results exhibited that the developed biosensor showed no obvious response to Lys, Ig G or BSA, while significant fluorescence restoration were observed in the present of thrombin. These results implied the sensor was

highly selective to its target and had excellent ability in resisting disturbance.

In summary, we have reported that the nanoassembly of aptamer probes on MoS_2 nanosheets retained the binding affinity and high selectivity of the aptamer to its target, and binding of the aptamer to the target released the aptamer probe away from the MoS_2 nanosheet. Using aptamer probes with single fluorophore label in the nano-assembly, we have developed a novel fluorescence-activated DNA-MoS_2 nanosheet biosensor for protein and small molecule targets. This nanobiosensor can be prepared very easily, allowing single-step and rapid detection, showing high sensitivity and signal-to-backgorund, and exhibiting excellent selectivity. The DNA-MoS_2 nanosheet biosensor can be very versatile and easily extended to the detection of a wide range of targets by using different aptamers and possibly in multiplexed assays using multicolor fluorophore labels, which may create a new dimension for MoS_2 nanosheets in biomedical applications.

Notes and references

State Key Laboratory of Chemo/Bio-Sensing and Chemometrics, College of Chemistry and Chemical Engineering, Hunan University, Changsha, 410082, P. R. China, Tel: 86-731-88821916; Fax :86-731-88821916; E-mail: rqyu@hnu.edu.cn ; xiachu@hnu.edu.cn.

† Electronic Supplementary Information (ESI) available: Experimental details and additional Figures. See DOI: 10.1039/b000000x/

1 A. D. Ellington and J. W. Szostak, *Nature* ., 1990, **346**, 818-822.
2 D. L. Robertson and G. F. Joyce, *Nature* ., 1990, **344**, 467-468.
3 C. Tuerk, L. Gold, *Science*., 1990, **249**, 505-510.
4 M. Famulok, G. Mayer and M. Blind, *Acc. Chem. Res.*, 2000, **33**, 591-599.
5 S. D. Jayasena, *Clin. Chem.*, 1999, **45** , 1628-1650.
6 S. Tombelli, M. Minunni and M. Mascini, *Biosens. Bioelectron.*, 2005, **20**, 2424-2434.
7 C. H. Lu, H. H. Yang, C. L. Zhu, X. Chen and G. N. Chen, *Angew. Chem. Int. Ed.*, 2009, **48**, 4785-4787.
8 J. W. Liu, J. H. Lee and Y. Lu, *Anal. Chem.*, 2007, **79**, 4120-4125.
9 S. Schachermeyer, J. Ashby and W. W. Zhong, *J. Chromatogr. A.*, 2013, **1295**, 107-113.
10 W. H. Tan, M. J. Donovan and J. H. Jiang, *Chem. Rev*., 2013, **113**, 2842-2862.
11 S. J. Zhen, L. Q. Chen, S. J. Xiao, Y. F. Li, P. P. Hu, L. Zhan, L. Peng, E. Q. Song and C. Z. Huang, *Anal. Chem*., 2010, **82**, 8432-8437.
12 J. Zhang, L. H. Wang, H. Zhang, F. Boey, S. P. Song and C. H. Fan, *Small*., 2010, **6**, 201-204.
13 C. Y. Zhang and L. W. Johnson, *Anal. Chem*., 2009, **81**, 3051-3055.
14 Z. W. Tang, P. Mallikaratchy, R. H. Yang, Y. M. Kim, Z. Zhu, H. Wang and W. H. Tan, *J. Am. Chem. Soc*., 2008, **130**, 11268-11269.
15 B. R. Baker, R. Y. Lai, M. S. Wood, E. H. Doctor, A. J. Heeger and K. W. Plaxco, *J. Am. Chem. Soc*., 2006, **128**, 3138-3139.
16 Y. Xiao, B. D. Piorek, K. W. Plaxco and A. J. Heeger, *J. Am. Chem. Soc*., 2005, **127**, 17990-17991.
17 F. Xia, X. L. Zuo, R. Q. Yang, Y. Xiao, D. Kang, A. Vallee-Belisle, X. Gong, J. D. Yuen, B. B. Y. Hsu, A. J. Heeger and K. W. Plaxco, *Proc. Natl. Acad. Sci. U.S.A*., 2010, **107**, 10837-10841.
18 M. N. Stojanovic and D. W. Landry, *J. Am. Chem. Soc*., 2002, **124**, 9678-9679.
19 Z. Y. Zeng, Z. Y. Yin, X. Huang, H. Li, Q. Y. He, G. Lu, F. Boey and H. Zhang, *Angew. Chem. Int. Ed.*, 2011, **50**, 11093-11097.
20 B. Radisavljevic, A. Radenovic, J. Brivio, V. Giacometti and A. Kis, *Nat. Nanotechnol*., 2011, **6**, 147-150.
21 H. Li, Z. Y. Yin, Q. Y. He, X. Huang, G. Lu, D. W. H. Fam, A. I. Y. Tok, Q. Zhang and H. Zhang, *Small*., 2012, **8**, 63-67.
22 Z. Y. Yin, H. Li, L. Jiang, Y. M. Shi, Y. H. Sun, G. Lu, Q. Zhang, X. D. Chen and H. Zhang, *ACS. Nano*., 2012, **6**, 74-80.
23 W. J. Zhou, Z. Y. Yin, Y. P. Du, X. Huang, Z. Y. Zeng, Z. X. Fan, H. Liu, J. Y. Wang and H. Zhang, *Small*., 2013, **9**, 140-147.
24 Q. Y. He, Z. Y. Zeng, Z. Y. Yin, H. Li, S. X. Wu, X. Huang and H. Zhang, *Small*.**,** 2012, **8**, 2994-2999.
25 C. F. Zhu, Z. Y. Zeng, H. Li, F. Li, C. H. Fan and H. Zhang, *J. Am. Chem. Soc.*, 2013, **135**, 5998-6001.
26 G. Eda, H. Yamaguchi, D. Voiry, T. Fujita, M. W. Chen and M. Chhowalla, *Nano Lett.*, 2011, **11**, 5111-5116.
27 Y. Wang, Z. H. Li, T. J. Weber, D. H. Hu, C. T. Lin, J. H. Li and Y. H. Lin, *Anal Chem.*, 2013, **85**, 6775-6782.
28 R. H. Yang, Z. W.Tang, J. L.Yan, H. Z. Kang, Y. M. Kim, Z. Zhu and W. H.Tan, *Anal. Chem.*, 2008, 80, 7408-7413.